



Published in final edited form as:

Toxicol Appl Pharmacol. 2008 July 15; 230(2): 167–174. doi:10.1016/j.taap.2008.02.024.

Intracellular Localization and Subsequent Redistribution of Metal Transporters in a Rat Choroid Plexus Model Following Exposure to Manganese or Iron

Xueqian Wang^{a,1}, David S. Miller^b, and Wei Zheng^{a*}

^aSchool of Health Sciences, Purdue University, West Lafayette, IN 47907

^bNIH/NIEHS, Research Triangle Park, NC 27709, USA

Abstract

Confocal microscopy was used to investigate the effects of manganese (Mn) and iron (Fe) exposure on the subcellular distribution of metal transporting proteins, i.e., divalent metal transporter 1 (DMT1), metal transporter protein 1 (MTP1), and transferrin receptor (TfR), in the rat intact choroid plexus which comprises the blood-cerebrospinal fluid barrier. In control tissue, DMT1 was concentrated below the apical epithelial membrane, MTP1 was diffuse within the cytosol, and TfR was distributed in vesicles around nuclei. Following Mn or Fe treatment (1 and 10 μ M), the distribution of DMT1 was not affected. However, MTP1 and TfR moved markedly toward the apical pole of the cells. These shifts were abolished when microtubules were disrupted. Quantitative RT-PCR and Western blot analyses revealed a significant increase in mRNA and protein levels of TfR but not DMT1 and MTP1 after Mn exposure. These results suggest that early events in the tissue response to Mn or Fe exposure involve microtubule-dependent, intracellular trafficking of MTP1 and TfR. The intracellular trafficking of metal transporters in the choroid plexus following Mn exposure may partially contribute to Mn-induced disruption in Fe homeostasis in the cerebrospinal fluid (CSF) following Mn exposure.

Keywords

cerebrospinal fluid; blood-cerebrospinal fluid barrier; confocal microscopy; manganese; iron; divalent metal transporter; transferrin receptor; metal transporter protein

Introduction

Chemical homeostasis of brain extracellular fluid is maintained by two major barrier systems, i.e., the blood-brain barrier (BBB) that separates blood from brain interstitial fluid and the blood-cerebrospinal fluid barrier (BCB) that separates blood from cerebrospinal fluid (CSF). Both barriers selectively allow essential nutrients, metal ions and drug molecules to enter the brain parenchyma and selectively remove metabolic wastes and potential toxicants from brain extracellular fluid. The BCB resides within the choroid plexus, a polarized epithelium with the

*To whom all correspondences should be addressed: Wei Zheng, Ph.D., Purdue University School of Health Sciences, 550 Stadium Mall Drive, Room 1163D, West Lafayette, IN 47907, Phone: 765 496-6447, Fax: 765 496-1377, E-mail: wz18@purdue.edu.

¹Current address: NIH/NIEHS, Research Triangle Park, NC 27709, USA

Publisher's Disclaimer: This is a PDF file of an unedited manuscript that has been accepted for publication. As a service to our customers we are providing this early version of the manuscript. The manuscript will undergo copyediting, typesetting, and review of the resulting proof before it is published in its final citable form. Please note that during the production process errors may be discovered which could affect the content, and all legal disclaimers that apply to the journal pertain.

basolateral surface facing the blood and the apical brush border surface in direct contact with CSF. The choroid plexus epithelium plays an important role modulating movement of chemicals including metal ions between blood and CSF (Zheng *et al.* 2003).

Disrupted brain iron (Fe) homeostasis leading to an Fe-initiated overproduction of reactive oxygen species and the ensuing lipid peroxidation has been associated with the etiology of Parkinson's disease (Double *et al.* 2000; Berg *et al.* 2001; Jenner, 2003). Previous studies from this laboratory reveal that CSF Fe concentration is partly regulated by the choroid plexus. Subchronic exposure to the toxic metal, manganese (Mn), alters Fe homeostasis in the CSF, possibly by affecting one or more facilitated transport mechanisms in choroid plexus (Zheng *et al.* 1999; Zheng and Zhao, 2001; Li *et al.* 2005; Wang *et al.* 2006). In this regard, three putative Fe transporters, i.e., divalent metal transporter-1 [DMT1, also know as divalent cation transporter 1 (DCT1), or natural resistance-associated macrophage protein 2 (Nramp2)], metal transporter protein-1 [MTP1, also described as iron-regulated transporter 1 (IREG1), ferroportin 1, or SLC11A3 Fe transporter], and transferrin receptor (TfR), have been shown to be expressed in choroid plexus (Giometto *et al.* 1990; Gunshin *et al.* 1997; Wu *et al.* 2004). The mRNA transcripts of all three transporters contain a stem-loop structure known as iron responsive element (IRE), which is located at 3'-untranslated region (UTR) of DMT1 or TfR mRNA transcripts and at 5'- UTR of MTP1 mRNA transcripts. This unique IRE-containing mRNA structure allows binding of cytosolic iron-regulatory protein-1 (IRP1) to mRNAs, providing fine regulation of the expression of these Fe transporters (Klausner *et al.* 1993; Andrews, 1999; Gunshin *et al.* 2001).

Available information indicates that each of the Fe transporters performs a different function within cells. TfR is a transmembrane glycoprotein consisting of two 90-kDa subunits each of which binds one transferrin molecule. TfR mediates cellular uptake of transferrin-bound Fe, which in most cells is by receptor-mediated endocytosis. Within cells, Fe is believed to be released from the transferrin-TfR complex in acidified endosomes with free ferric Fe reduced to ferrous Fe by ferrireductase (Bali *et al.* 1991; Sipe and Murphy, 1991). At the apical surface of absorptive cells in the duodenum, DMT1 functions to transport a number of divalent metal ions including Mn, Fe, copper (Cu), zinc (Zn) and cobalt (Co) into the cells by proton/metal symport (Gunshin *et al.* 1997). MTP1 has been localized to the inner cell surface of enterocytes, macrophages, hepatocytes and placental membrane, where it appears to mediate metal efflux (Abboud and Haile, 2000; Donovan *et al.* 2000; McKie *et al.* 2000).

All three of these metal transporters are expressed in choroid plexus, providing potential sites of physiological and pathological regulation of Fe homeostasis in the central nervous system by other metals (Giometto *et al.* 1990; Gunshin *et al.* 1997; Wu *et al.* 2004). Indeed, it has been suggested that abnormally high expression of TfR and DMT1 in the BCB could lead to an abnormally elevated Fe concentrations in the CSF of Mn-exposed animals (Zheng *et al.* 1999; Li *et al.* 2005). Previous studies with cultured choroidal epithelial cells showed that Mn exposure, enhances binding of IRP1 to IRE-containing mRNAs and increases expression of DMT1 and TfR (Zheng *et al.* 1999; Li *et al.* 2005; Wang *et al.* 2006). In this regard, the present study is focused on the effects of Mn and Fe exposure on the subcellular location and expression of DMT1, MTP1 and TfR in the rat choroid plexus, which may contribute to Mn-induced disruption of Fe homeostasis in Mn Parkinsonism.

Methods

Materials

Rabbit anti-rat-DMT1 antibody and rabbit anti-rat-MTP1 antibody was obtained from Alpha Diagnostic International (San Antonio, CA), mouse anti-human TfR antibody from ZYMED Laboratories Inc. (South San Francisco, CA), and Alexa-labeled secondary antibodies from

Molecular Probes (Eugene, OR). The specificity and selectivity of these antibodies have been tested in our previous publications (Li et al., 2005; Wang et al., 2006). The enhanced chemiluminescence reagent (ECL) and ECL film were purchased from Amersham Biosciences (Piscataway, NJ). β -actin, dithiothreitol (DTT), 2-mercaptoethanol, phenylmethylsulfonyl fluoride (PMSF), polyacrylamide, tetramethyl-ethylenediamine (TEMED) and all chemicals were from Sigma Chemicals (St. Louis, MO). All reagents were of analytical grade, HPLC grade or the best available pharmaceutical grade.

Animals and treatment

Adult male Sprague-Dawley rats (250–300g) were euthanized by CO₂ inhalation. The top of the cranium was removed and choroid plexus tissue from both lateral ventricles was removed using a Dumont No. 5 forceps inserted into each hemisphere. Tissues were immediately transferred to an ice-cold, per-gassed (95% O₂-5% CO₂) artificial cerebrospinal fluid (aCSF) consisting of (in mM) 103 NaCl, 4.7 KCl, 2.5 CaCl₂, 1.2 KH₂PO₄, 1.2 MgSO₄, 25 NaHCO₃, 10 glucose, and 1 sodium pyruvate at pH 7.4 (Breen *et al.* 2002). For Mn or Fe treatment, each plexus was incubated with shaking in the aCSF containing 1, 10, and 100 μ M MnCl₂ or FeSO₄ for 1 hr at 37°C. In some experiments, choroid plexus tissues were also pre-treated with microtubule inhibitor-nocodazole (10 μ M) or microfilament inhibitor-cytochalasin D (1 μ M) for 10-min (Miller *et al.*, 1999) to examine the role of cytoskeleton in Mn-induced transport trafficking. During all treatments, the aCSF was under a constant flow of 95% O₂-5% CO₂.

Immunocytochemistry

Choroid plexus tissues were fixed with 3% paraformaldehyde/ 0.25% glutaraldehyde in phosphate buffered saline (PBS) for 10 min and permeabilized with 0.5% Triton X-100 for 30 min at room temperature followed by 5 washes with PBS. After blocking with 1% bovine serum albumin (BSA) in PBS for 30 min at room temperature, tissues were incubated with rabbit anti-DMT1 (1:10), rabbit anti-MTP1 (1:10) or mouse anti-TfR antibody (against DMT1 isoform I with IRE at transcripts) (1:100) in 1% BSA at 37°C for 60 min, washed with PBS with 1% BSA, and then incubated with Alexa-488 conjugated secondary antibody (1:500) in 1% BSA at 37°C for 60 min. After further washing in PBS with 1% BSA, tissue was transferred to covered Teflon microscope imaging chamber (Breen *et al.* 2002) for confocal microscopy. Negative controls were treated similarly except they were not exposed to primary antibody.

Confocal immunofluorescence microscopy

To acquire images, the chamber containing the specimen was mounted on the stage of a Zeiss Model 510 inverted confocal laser-scanning microscope and viewed through a 40x water-immersion objective (numeric aperture=1.2), with a 488-nm laser line for excitation (Ar-ion laser), a 505 nm dichroic filter and a 510-nm long-pass emission filter. Low laser intensity was used to avoid photobleaching. First, tissues were examined under reduced transmitted-light illumination and an area containing undamaged epithelium and underlying vasculature was selected. Confocal images (512 \times 512 \times 8 bits, 4 frames averaged) were acquired and saved to disk. For each tissue sample, 5–10 areas of epithelium were selected for image collection. Data reported are the results of single experiments that are representative of three to four replicate experiments.

Quantitative real-time RT-PCR analyses

Levels of DMT1, MTP1 and TfR mRNA were quantified using real-time RT-PCR as described previously (Walker, 2001; Wang *et al.*, 2006). Briefly, total RNA was isolated from rat choroid plexus tissues using Tri-Reagent following the manufacturer's direction (Molecular Research Center, Cincinnati, OH). An aliquot (1 μ g) of RNA was reverse-transcribed with MuLV reverse transcriptase (Applied Biosystems, Foster City, CA) and oligo-dT primers. The forward and

reverse primers for selected genes were designed using Primer Express 2.0 software (Applied Biosystems, Foster City, CA). The Absolute QPCR SYBR green Mix kit (ABgene, Rochester, New York) was used for real-time RT-PCR. Amplification was carried out in the Mx3000P Real-Time PCR System (Stratagene, La Jolla, CA). PCR run began with an activation step of 95°C for 15 min that was compatible with a hot start action. The PCR amplification phase consisted of 40 cycles of amplification using a plateau of 95°C for 30 sec for denaturation, followed by a plateau of 60°C for 1 min for annealing, and a plateau of 72°C for 30 sec for extension. A dissociation curve was used to verify that the majority of fluorescence detected could be attributed to the labeling of specific PCR products, and to verify the absence of primer-dimers and sample contamination. All real time RT-PCR reactions were done in triplicate.

Primers sequences used for real-time RT-PCR were: for rat DMT1 using a forward primer 5'-CAG TGC TCT GTA CGT AAC CTG TAA GC-3' and a reverse primer 5'-CGC AGA AGA ACG AGG ACC AA -3' (Genbank Accession No. AF008439), which amplify one isoform of DMT1 containing IRE; for rat MTP1 using a forward primer 5'-CCA CCT GTG CCT CCC AGA T-3' and a reverse primer 5'-CCC ATG CCA GCC AAAAAT AC - 3' (Genbank Accession No. AF394785); for rat TfR using a forward primer 5'-CTA GTA TCT TGA GGT GGG AGG AAG AG-3' and a reverse primer 5'-GAG AAT CCC AGT GAG GGT CAG A -3' (Genbank Accession No. M58040); for rat glyceraldehydes-3-phosphate dehydrogenase (GAPDH), used as an internal control, using a forward primer 5'-CCT GGA GAA ACC TGC CAA GTA T-3' and a reverse primer 5'-AGC CCA GGA TGC CCT TTA GT-3' (Genbank Accession No. NM_017008). All the primers were synthesized from Sigma (Woodlands, TX).

The relative differences in gene expression between groups were expressed using cycle time (Ct) values. The Ct values of interested genes were first normalized with that of GAPDH in the same sample; the relative differences between control and treatment groups were then calculated and expressed as relative increases by setting the control as 100%. Assuming that the Ct value is reflective of the initial starting copy and that there is 100% efficiency, a difference of one cycle is equivalent to a two-fold difference in starting copy (Li *et al.* 2006; Wang *et al.* 2006).

Western blot analyses of DMT1, MTP1 and TfR

Western blot experiments were carried out as described previously (Wang *et al.* 2006). In short, following incubation, choroid plexus tissues were homogenized (1:10, wt/vol) on ice in a buffer containing 20 mM Tris (pH 7.5), 5 mM EGTA, 1% TritonX-100, 0.1% SDS, 50µM phenylmethylsulphonylfluoride (PMSF), 15 mM 2-mercaptoethanol and a Protease Inhibitor Cocktail, composed of 500 µM 4-(2-Aminoethyl) benzenesulfonyl fluoride hydrochloride (AEBSF), 150 nM aprotinin, 1µM E-64, 0.5 mM EDTA, 1µM leupeptin (Calbiochem, San Diego, CA). Samples were sonicated using Sonifer Model 250 at duty cycle 20% and output 4–6 for 30 pulses. Following centrifugation at 10,000g at 4°C for 10 min, aliquots of supernatants were assayed for protein concentrations by the Bradford method. A volume of protein extract (50 µg of protein) was mixed with an equal volume of 6X sample buffer (0.35 M Tris-Cl, 10% SDS, 30% glycerol, 0.6 M DTT, 0.012% bromophenol blue), loaded onto a 10% SDS-polyacrylamide gel, electrophoresed, and then transferred to a PVDF membrane. The membrane was blocked with 5% dry milk in TBST (Tris-buffered saline) at room temperature for 1 hr and immunoblotted with an antibody directly against DMT1 with IRE (1:500) or rabbit anti-rat-MTP1 antibody (1:500) or mouse TfR antibody (1:500). The membrane was stained with a horse-radish peroxidase (HRP)-conjugated goat anti-rabbit IgG or anti-mouse antibody (1:2000) at room temperature for 1 hr and developed using ECL reagent and films. The exposure time varied from 30 sec to a few min depending on signal strength. β -actin (42 kD) (1:2000) was used as an loading control; the corresponding secondary antibody (1:3000) for β -actin was HRP-conjugated goat anti-mouse IgG. Band intensities were

quantified using UN-SCAN-IT™ (Version 5.1) software (Silk Scientific Inc., Orem, Utah). Western blotting for all three transporters were done in triplicates.

Statistical analysis

All data are expressed as mean \pm SEM. The replicates of experiments conducted in the same animal were referred as n=1; data from three or four animals were used for statistical analyses. Statistical analyses of the differences between groups were carried out by one-way ANOVA using the SPSS 12.0 statistics package for Windows. Differences between two means were considered significant when *p* was equal or less than 0.05.

Results

DMT1, MTP1 and TfR are expressed in rat choroid plexus tissues from immunocytochemistry

Immunocytochemistry in rat choroid plexus tissue revealed distinct staining patterns for the three Fe transporters (Fig. 1). Staining for all three transporters was primarily intracellular, with only limited signal evident on the apical plasma membrane. No staining was found within nuclei. For DMT1, immunofluorescence was localized primarily in the region between the nucleus and the apical plasma membrane (Fig. 1A). Staining for MTP1 seemed to be more diffuse and less polarized. Some signal was also found on the outer edge of the apical brush membrane (Fig. 1B). Staining for TfR localized to the region around nuclei in what appeared to be clusters of vesicles (Fig. 1C). Low panel in Fig. 1 shows the corresponding transmission images indicating normal morphology of choroid plexus tissues.

Exposure to Mn or Fe alters the subcellular distribution of MTP1 and TfR, but not DMT1

DMT1, MTP1 and TfR, exhibited different responses to Mn or Fe treatment. Exposure of choroid plexus for 1 hr to 1 or 10 μ M Mn or Fe in aCSF did not noticeably affect the pattern of DMT1 staining (Fig. 2).

In contrast, Mn exposure caused a shift in the pattern of MTP1 staining. This transporter now concentrated in the cytoplasmic space between nuclei and the apical plasma membrane. A time course study indicated that the movement of MTP1 occurred within 30 min of 100 μ M Mn exposure; by 1 hr, nearly all of MTP1 staining was found beneath the apical, brush border membrane (data not shown). This shift was evident at aCSF Mn concentrations as low as 1 μ M and more pronounced with 10 μ M Mn (Fig. 3). With the latter Mn concentration, staining was visible within the microvilli of the apical plasma membrane (Fig. 3C). Exposure of choroid plexus tissue for 1 hr to 1 and 10 μ M Fe resulted in a similar shift of MTP1 staining to the apical cytoplasm (Fig. 3E, F). However, with Fe exposure, brush border staining was not as evident as with Mn exposure.

Exposure of choroid plexus tissue to 1–10 μ M Mn (1 hr) or 10 μ M (2 h) Fe also caused a shift in the staining pattern for TfR (Fig. 4). In controls, TfR was distributed in large, discrete structures surrounding the nucleus. With Mn or Fe exposure these structures remained perinuclear, but they had moved to the apical cytoplasm.

Nocodazole and cytochalasin D abolishes the redistribution of MTP1 and TfR

These shifts of TfR were abolished when tissue was pretreated with nocodazole, a disruptor of microtubules (Fig. 5) or cytochalasin D, a disruptor of the actin cytoskeleton, suggesting cytoskeletal involvement in the process. Similar inhibition of redistribution was also found for MTP1 (not shown). Neither nocodazole *nor* cytochalasin D affected the distribution of TfR or MTP1 in control tissue.

Mn exposure increases mRNA and protein levels of TfR, but not DMT1 or MTP1

Quantitative real-time RT-PCR was used to determine the effect of Mn exposure on mRNA levels of DMT1, MTP1 and TfR. The amounts of mRNA for these transporters were normalized to that of GAPDH mRNA in the corresponding samples. Unlike our previous observation from immortalized choroidal epithelial Z310 cells (Wang *et al.* 2006), Mn exposure did not affect the mRNA level of DMT1 in isolated rat choroid plexus tissues (Fig. 6), neither did it alter MTP1 mRNA levels. However, Mn treatment at 10 μ M for 1 hr significantly increased TfR mRNA by 6 folds ($p < 0.01$, Fig. 6). Protein expression of these transporters was analyzed by Western blot. Following treatment of choroid plexus tissues with 10 μ M of Mn for 1 hr, a significant increase (37%) in cellular protein levels of TfR was observed, but the protein levels of DMT1 and MTP1 were unchanged (Fig. 7A, B). Apparently, Mn exposure not only caused redistribution of TfR in the choroidal cells, but also increased the expression of TfR mRNA.

Discussion

In the present study, the immunostaining and confocal microscopy were first successfully used to visualize intracellular localization and translocation of three metal transport proteins in intact rat choroid plexus and to detect changes in their distribution after tissue was exposed to Mn or Fe. In tissue not exposed to metals, all three proteins were found within the epithelial cells. Both DMT1 and MTP1 were distributed diffusely within the cytoplasm, although for both one has the impression that they could have been contained in or on discrete structure, e.g., small vesicles (see for example Fig. 3). In contrast, TfR appeared to be within large vesicular structures that were distributed around nuclei. In control tissue, none of the metal transporting proteins exhibited detectable surface membrane localization as has been seen for DMT1 and MTP1 in other metal transporting tissues (Abboud and Haile, 2000; Tabuchi *et al.* 2002; Yang *et al.* 2002). Based on these findings, one might speculate that if the transport proteins are indeed functional in control tissue they play a role in the intracellular distribution or trafficking of substrates rather than a direct role in uptake and efflux from the cells.

In vitro exposure of choroid plexus tissue to micromolar concentrations of Mn and Fe in aCSF did not affect DMT1 distribution, DMT1 mRNA or protein. In contrast, metal exposure caused both MTP1 and TfR to move towards the apical (CSF) pole of the epithelial cells, with some MTP1 stain becoming evident within the brush border membrane. For both proteins, a microtubule-disrupting agent, nocodazole, abolished the metal-induced shifts, suggesting cytoskeletal involvement. Interestingly, of the three metal transport proteins, only TfR exhibited any change in expression following metal exposure; both mRNA and protein levels were significantly increased. Note that the measured increase in TfR protein was only 37% and this change appeared to be too small to be evident with immunostaining.

These observations are novel and generate several important questions regarding to the metal transporters in choroid plexus. First, what is the physiological consequence of intracellular redistribution of metal transporters and how may this contribute to an increased CSF Fe concentrations seen in our early in vivo studies (Zheng *et al.* 1999; Li *et al.* 2006)? Since DMT1 is primarily present in the apical side of the BCB facing the CSF, when the tissue was incubated with free Mn ions in the aCSF, DMT1 may function to take up metal ions in the CSF and transport them into the cells, leading to an elevated intracellular Mn concentration. The latter may trigger the intracellular trafficking of MTP1 toward the epithelial microvilli for the purpose of expelling the excess metal ions from the cells to the CSF as a part of the cell's defense mechanism against cellular overload of toxic metals (Fig. 8). The same mechanism may come into play when the cells were exposed to Fe in the aCSF. Interestingly, the direction of cellular MTP1 trafficking is not toward the blood, but rather uniquely toward the CSF side of the choroidal epithelia. Thus, the function of MTP1 in the BCB appears likely to be associated with its mobilization of metal ions from the blood to the CSF.

The shift of TfR stains to the apical side of the cells could be a result of the endocytosis of TfR following the binding of transferrin-bound metals to TfR in tissues. Since in the current study we did not use transferrin-bound Mn or Fe and there was no transferrin present in the aCSF, the intracellular redistribution of TfR seemed unlikely due to transferrin-bound metals, but rather the cell's response to free metal ions. Our previous studies have shown that the upregulation of TfR by Mn exposure can be achieved by enhanced binding of IRP1 to TfR 3'-UTR IRE-containing mRNA (Li *et al.* 2005). The active center of IRP1 contains a [4Fe-4S] cluster, with one labile Fe whose presence or absence in the cluster determines the IRP1 either as an Fe regulatory protein or as an enzyme involving in cellular energy production (Kennedy *et al.* 1983; Robbins and Stout, 1985). In the Fe-deficient condition, IRP1 binds with a high affinity to 3'-IRE containing TfR mRNAs, stabilizes the expression of this transporter, and increases intracellular levels of TfR (Eisenstein and Blemings, 1998; Wilkie *et al.* 2003). Toxic metal Mn may replace the fourth labile Fe in IRP1 structure, because Mn ions share several chemical and biochemical properties closely resembling Fe with regards to ionic radius, electrical charges in biological matrices, binding affinity to the carrier proteins, and subcellular accumulation in mitochondria (Zheng *et al.* 1998; Aschner *et al.* 1999; Chen *et al.* 2001). Consequently, the binding stabilizes the protein translation and thus increases TfR expression as observed in this and our previous studies (Zheng *et al.* 1999; Zheng and Zhao, 2001; Li *et al.* 2004; Li *et al.*, 2005). The move of TfR toward the apical side of the choroidal epithelia may reflect TfR's function to transport transferrin-bound Fe or Mn from an endogenously available transferrin pool. It is interesting to note that similar to MTP1, the direction of cellular TfR trafficking was toward the CSF. The difference may be that MTP1 expels excessive intracellular free metal ions while TfR moves intracellular transferrin-bound metals to the CSF.

Fig. 8 illustrates the postulated regulatory mechanism. Upon Mn exposure from the CSF, the apical DMT1 may take up the metal from the aCSF into the cells. As a protective measure, MTP1 reacts to expel overloaded Mn back to the CSF. Elevated intracellular Mn concentration, on the other hand, increases the translational expression of TfR by interacting with the [Fe-S] cluster of IRPs, leading to a TfR-mediated intracellular transport of transferrin-bound metals including Fe to the CSF. The endpoint of transporters' intracellular trafficking is the reduction of Fe uptake from the CSF and an increase of Fe in the CSF. Our recent ventriculo-cisternal brain perfusion study performed on sub-chronically Mn-exposed rats (6 mg Mn/kg ip for 30 days) revealed a declined uptake of infused ⁵⁹Fe by the choroid plexus and an increased Fe level in the CSF outflow (data unpublished; manuscript in preparation). Thus, the intracellular trafficking of these transporters may explain, at least partially, a preferred direction of Fe transport, from the blood to the CSF, by the BCB, as the similar translocation has been reported in intestine (Ma *et al.* 2006).

It is also possible that the redistribution of these transporters in the cytoplasm is the cell's response in order to sequester excess metals from the CSF. With the increase of Mn/Fe concentrations in the CSF, TfR may become functionally active through the process of involving itself in moving transferrin-bound Fe in the cells. The released metal ions from TfR or free cellular ions are then further acquired by MTP1, favored by its presence on the microvilli. As a consequence, excess metal stress in the CSF may be relieved by the coordinated translocation of these transporters as a part of the defense mechanism to protect the homeostasis of the CSF.

The second important implication from this study is the subcellular redistribution of these transporters. Previously in rat choroid plexus studies, the release of quinacrine-loaded vesicles is markedly reduced by microtubule disruptor nocodazole (Miller *et al.* 1999). In the current study, pretreatment of choroid plexus tissues with nocodazole and cytochalasin D (a microfilament inhibitor) effectively blocked Mn exposure-induced intracellular trafficking of TfR and MTP1, respectively. This observation indicates that both microtubules and

microfilaments are involved in the subcellular redistribution of metal transporters. The questions as to how metals activate microtubules and microfilaments, what signals guide the direction of transporters' trafficking, and whether or not it is associated with the regulation in IRE-containing mRNAs, are unanswered and deserve further investigation.

Noticeably, the early changes we observed in these proteins may only be initial events that may not be related to the final states of transport. More research is needed to explore the involvement of other transporters in the final transport characteristics of the tissue. Furthermore, freshly extracted choroid plexus tissues used in the present study provides an intact choroid plexus structure, which is ideal for epithelial uptake studies. However, this may not be a direct reflection of animal tests due to the differences between in vitro and in vivo study.

In conclusion, our study demonstrates that under the normal physiological condition, MTP1 in the blood-CSF barrier of the choroid plexus functions to transport excess amounts of Mn or Fe from the cells to the CSF. TfR appears to transport transferrin-bound Mn or Fe from the blood toward the CSF. Following Mn or Fe treatment, the redistribution of MTP1 and TfR in the choroidal epithelia were distributed toward the CSF. The effect of Mn on TfR overexpression and translocation seems likely to be mediated by increased translational expression of TfR. The unique intracellular trafficking of metal transporters toward the CSF side of the BCB following Mn exposure may underlie Mn-induced Fe imbalance between the blood and the CSF.

Acknowledgments

We are grateful to Dr. Bjoern Bauer (NIH/NIEHS) for his technical assistance in confocal microscopy and Ms. Destiny B. Sykes (NIH/NIEHS) for her kind help in animal dissection. This study was supported by NIH/National Institute of Environmental Health Sciences grants RO1 ES008146 and R21 ES013118.

References

- Abboud S, Haile DJ. A novel mammalian iron-regulated protein involved in intracellular iron metabolism. *J Biol Chem* 2000;275:19906–19912. [PubMed: 10747949]
- Andrews NC. The iron transporter DMT1. *Int J Biochem Cell Biol* 1999;31:991–994. [PubMed: 10582331]
- Aschner M, Vrana KE, Zheng W. Manganese uptake and distribution in the central nervous system (CNS). *Neurotoxicology* 1999;20:173–180. [PubMed: 10385881]
- Bali PK, Zak O, Aisen P. A new role for the transferrin receptor in the release of iron from transferrin. *Biochemistry* 1991;30:324–328. [PubMed: 1988034]
- Berg D, Gerlach M, Youdim MB, Double KL, Zecca L, Riederer P, Becker G. Brain iron pathways and their relevance to Parkinson's disease. *J Neurochem* 2001;79:225–236. [PubMed: 11677250]
- Breen CM, Sykes DB, Fricker G, Miller DS. Confocal imaging of organic anion transport in intact rat choroid plexus. *Am J Physiol Renal Physiol* 2002;282:F877–F885. [PubMed: 11934698]
- Chen JY, Tsao GC, Zhao Q, Zheng W. Differential cytotoxicity of Mn(II) and Mn(III): special reference to mitochondrial [Fe-S] containing enzymes. *Toxicol Appl Pharmacol* 2001;175:160–168. [PubMed: 11543648]
- Donovan A, Brownlie A, Zhou Y, Shepard J, Pratt SJ, Moynihan J, Paw BH, Drejer A, Barut B, Zapata A, Law TC, Brugnara C, Lux SE, Pinkus GS, Pinkus JL, Kingsley PD, Palis J, Fleming MD, Andrews NC, Zon LI. Positional cloning of zebrafish ferroportin 1 identifies a conserved vertebrate iron exporter. *Nature* 2000;403:776–781. [PubMed: 10693807]
- Double KL, Gerlach M, Youdim MB, Riederer P. Impaired iron homeostasis in Parkinson's disease. *J Neural Transm Suppl* 2000:37–58. [PubMed: 11205155]
- Eisenstein RS, Blemings KP. Iron regulatory proteins, iron responsive elements and iron homeostasis. *J Nutr* 1998;128:2295–2298. [PubMed: 9868172]

- Giometto B, Bozza F, Argentiero V, Gallo P, Pagni S, Piccinno MG, Tavolato B. Transferrin receptors in rat central nervous system. An immunocytochemical study. *J Neurol Sci* 1990;98:81–90. [PubMed: 2230832]
- Gunshin H, Allerson CR, Polycarpou-Schwarz M, Rofts A, Rogers JT, Kishi F, Hentze MW, Rouault TA, Andrews NC, Hediger MA. Iron-dependent regulation of the divalent metal ion transporter. *FEBS Lett* 2001;509:309–316. [PubMed: 11741608]
- Gunshin H, Mackenzie B, Berger UV, Gunshin Y, Romero MF, Boron WF, Nussberger S, Gollan JL, Hediger MA. Cloning and characterization of a mammalian proton-coupled metal-ion transporter. *Nature* 1997;388:482–488. [PubMed: 9242408]
- Jenner P. Oxidative stress in Parkinson's disease. *Ann Neurol* 2003;53:S26–S36. [PubMed: 12666096] discussion S36-28
- Kennedy MC, Emptage MH, Dreyer JL, Beinert H. The role of iron in the activation-inactivation of aconitase. *J Biol Chem* 1983;258:11098–11105. [PubMed: 6309829]
- Klausner RD, Rouault TA, Harford JB. Regulating the fate of mRNA: the control of cellular iron metabolism. *Cell* 1993;72:19–28. [PubMed: 8380757]
- Li GJ, Choi BS, Wang X, Liu J, Waalkes MP, Zheng W. Molecular mechanism of distorted iron regulation in the blood-CSF barrier and regional blood-brain barrier following in vivo subchronic manganese exposure. *Neurotoxicology* 2006;27:737–744. [PubMed: 16545456]
- Li GJ, Zhang LL, Lu L, Wu P, Zheng W. Occupational exposure to welding fume among welders: alterations of manganese, iron, zinc, copper, and lead in body fluids and the oxidative stress status. *J Occup Environ Med* 2004;46:241–248. [PubMed: 15091287]
- Li GJ, Zhao Q, Zheng W. Alteration at translational but not transcriptional level of transferrin receptor expression following manganese exposure at the blood-CSF barrier in vitro. *Toxicol Appl Pharmacol* 2005;205:188–200. [PubMed: 15893546]
- Ma Y, Yeh M, Yeh KY, Glass J. Iron Imports. V. Transport of iron through the intestinal epithelium. *Am J Physiol Gastrointest Liver Physiol* 2006;290:G417–G422. [PubMed: 16474007]
- McKie AT, Marciari P, Rolfs A, Brennan K, Wehr K, Barrow D, Miret S, Bomford A, Peters TJ, Farzaneh F, Hediger MA, Hentze MW, Simpson RJ. A novel duodenal iron-regulated transporter, IREG1, implicated in the basolateral transfer of iron to the circulation. *Mol Cell* 2000;5:299–309. [PubMed: 10882071]
- Miller DS, Villalobos AR, Pritchard JB. Organic cation transport in rat choroid plexus cells studied by fluorescence microscopy. *Am J Physiol* 1999;276:C955–C968. [PubMed: 10199828]
- Robbins AH, Stout CD. Iron-sulfur cluster in aconitase. Crystallographic evidence for a three-iron center. *J Biol Chem* 1985;260:2328–2333. [PubMed: 3972791]
- Sipe DM, Murphy RF. Binding to cellular receptors results in increased iron release from transferrin at mildly acidic pH. *J Biol Chem* 1991;266:8002–8007. [PubMed: 2022630]
- Tabuchi M, Tanaka N, Nishida-Kitayama J, Ohno H, Kishi F. Alternative splicing regulates the subcellular localization of divalent metal transporter 1 isoforms. *Mol Biol Cell* 2002;13:4371–4387. [PubMed: 12475959]
- Walker NJ. Real-time and quantitative PCR: applications to mechanism-based toxicology. *J Biochem Mol Toxicol* 2001;15:121–127. [PubMed: 11424221]
- Wang X, Li GJ, Zheng W. Upregulation of DMT1 expression in choroidal epithelia of the blood-CSF barrier following manganese exposure in vitro. *Brain Res* 2006;1097:1–10. [PubMed: 16729984]
- Wilkie GS, Dickson KS, Gray NK. Regulation of mRNA translation by 5'- and 3'-UTR-binding factors. *Trends Biochem Sci* 2003;28:182–188. [PubMed: 12713901]
- Wu LJ, Leenders AG, Cooperman S, Meyron-Holtz E, Smith S, Land W, Tsai RY, Berger UV, Sheng ZH, Rouault TA. Expression of the iron transporter ferroportin in synaptic vesicles and the blood-brain barrier. *Brain Res* 2004;1001:108–117. [PubMed: 14972659]
- Yang F, Liu XB, Quinones M, Melby PC, Ghio A, Haile DJ. Regulation of reticuloendothelial iron transporter MTP1 (Slc11a3) by inflammation. *J Biol Chem* 2002;277:39786–39791. [PubMed: 12161425]
- Zheng W, Aschner M, Ghersi-Egea JF. Brain barrier systems: a new frontier in metal neurotoxicological research. *Toxicol Appl Pharmacol* 2003;192:1–11. [PubMed: 14554098]

- Zheng W, Ren S, Graziano JH. Manganese inhibits mitochondrial aconitase: a mechanism of manganese neurotoxicity. *Brain Res* 1998;799:334–342. [PubMed: 9675333]
- Zheng W, Zhao Q. Iron overload following manganese exposure in cultured neuronal, but not neuroglial cells. *Brain Res* 2001;897:175–179. [PubMed: 11282372]
- Zheng W, Zhao Q, Slavkovich V, Aschner M, Graziano JH. Alteration of iron homeostasis following chronic exposure to manganese in rats. *Brain Res* 1999;833:125–132. [PubMed: 10375687]

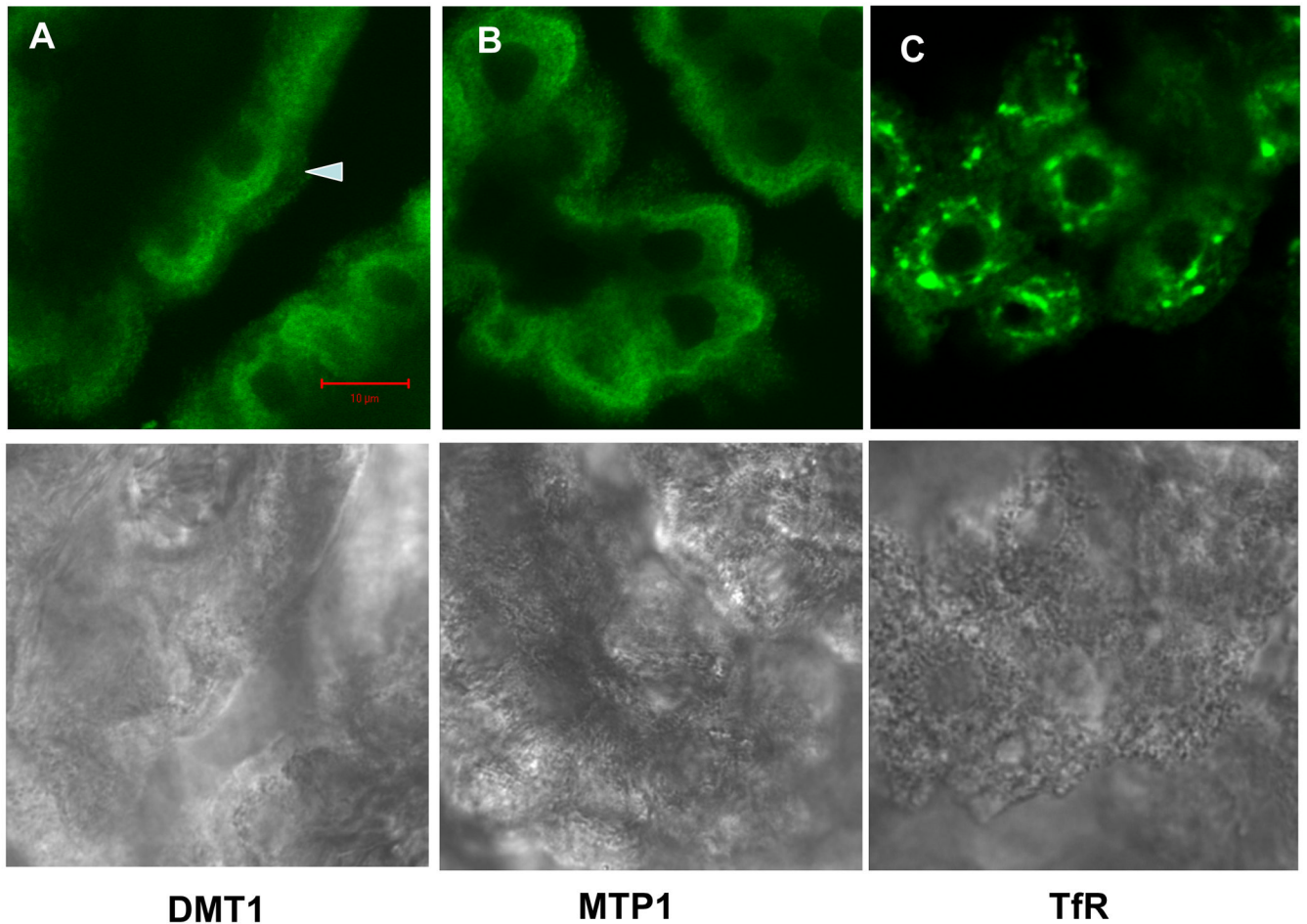


Fig. 1. Immunohistochemical staining of DMT1, MTP1 and TfR in rat choroid plexus tissues. DMT1 was cytosol-distributed, much along the apical side as the arrow showed; MTP1 was diffusive in the cytoplasm and some on the brush border; and TfR was localized around nuclei in the form of clusters. None of them existed in the nucleus. Lower panel showed corresponding transmission image, indicating normal morphology of choroid plexus tissues

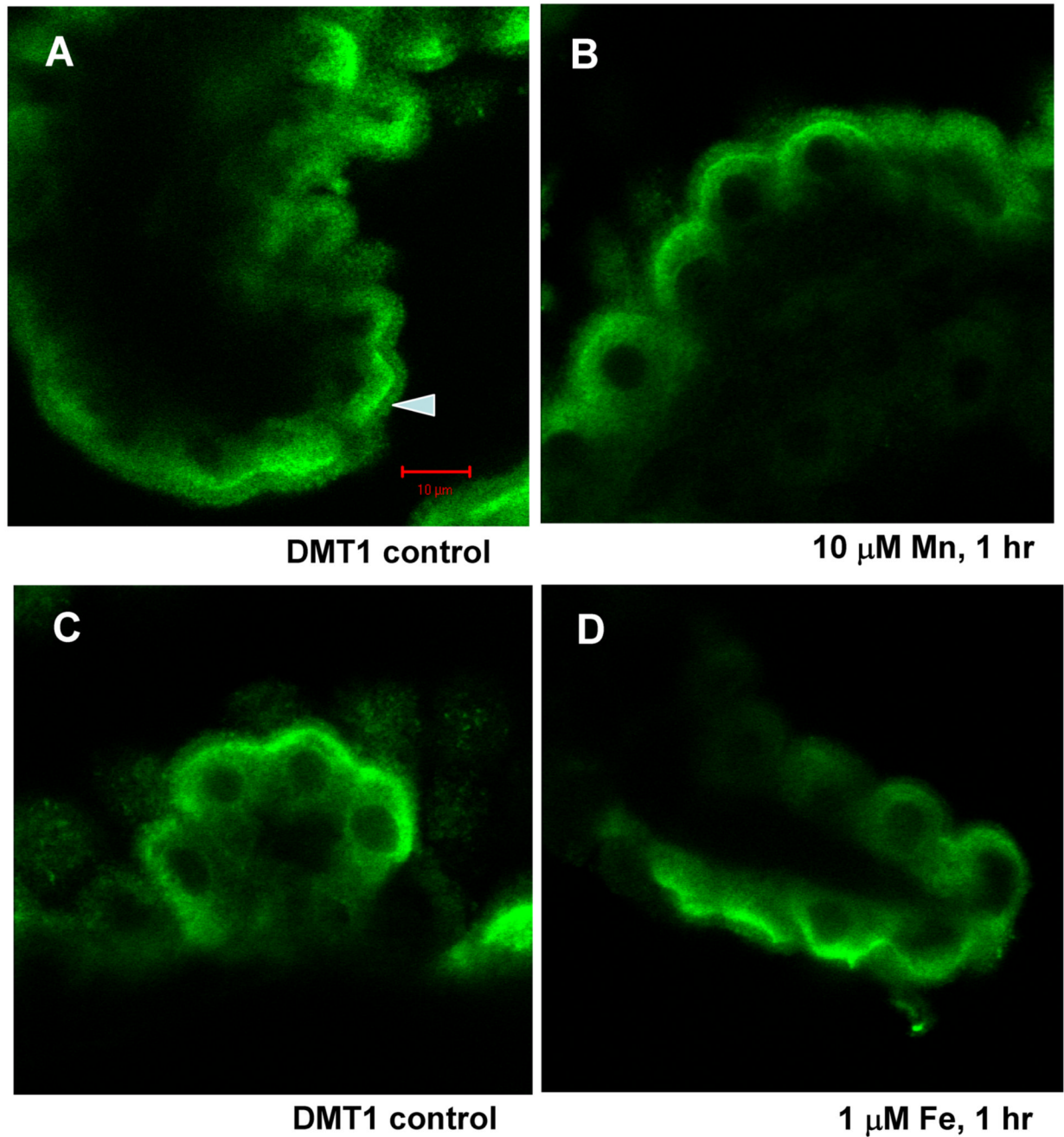


Fig. 2. Confocal study of DMT1 cellular distribution in rat choroid plexus tissues as affected by treatment with 0, 10 μM Mn (A and B) or 0, 1 μM Fe (C and D) for 1 hr. Tissues were immunostained with anti-DMT1 antibody. The distribution of DMT1 did not change following Mn or Fe incubation at concentrations tested.

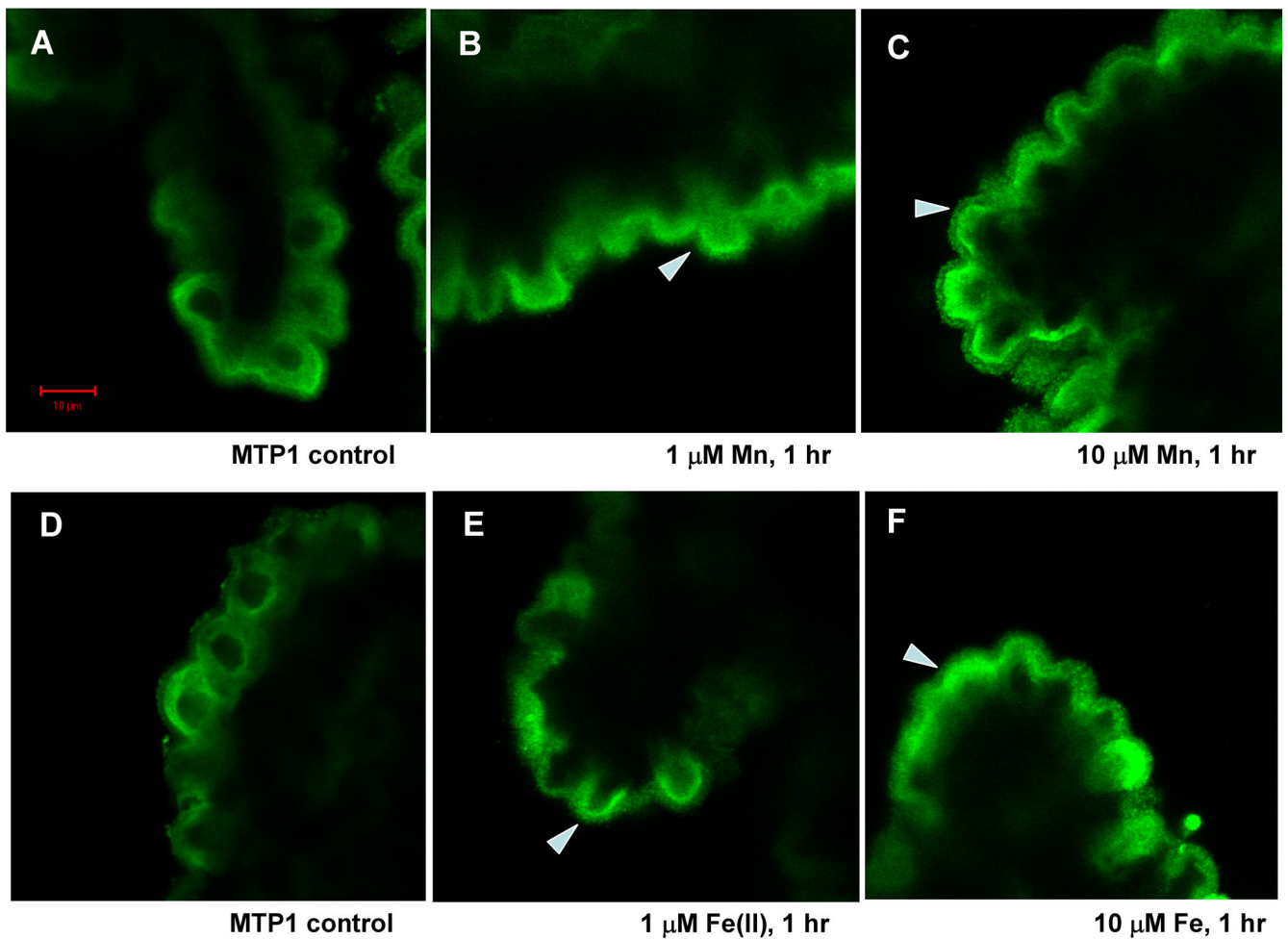


Fig. 3. Confocal study of MTP1 cellular distribution in rat choroid plexus tissues as affected by treatment with 0, 1 and 10 μM Mn (A, B, C) or Fe (D, E, F) for 1 hr. Tissues were immunostained with anti-MTP1 antibody. Following 1 μM Mn exposure, MTP1 stain moved towards the apical pole of the choroidal epithelia. At 10 μM Mn exposure, MTP1 stain on the brush border was intensified (see the arrow). Fe treatment resulted in the similar, yet less intensive redistribution of MTP1 in comparison to Mn treatment. Arrows indicated MTP1 redistribution of in response to Mn or Fe.

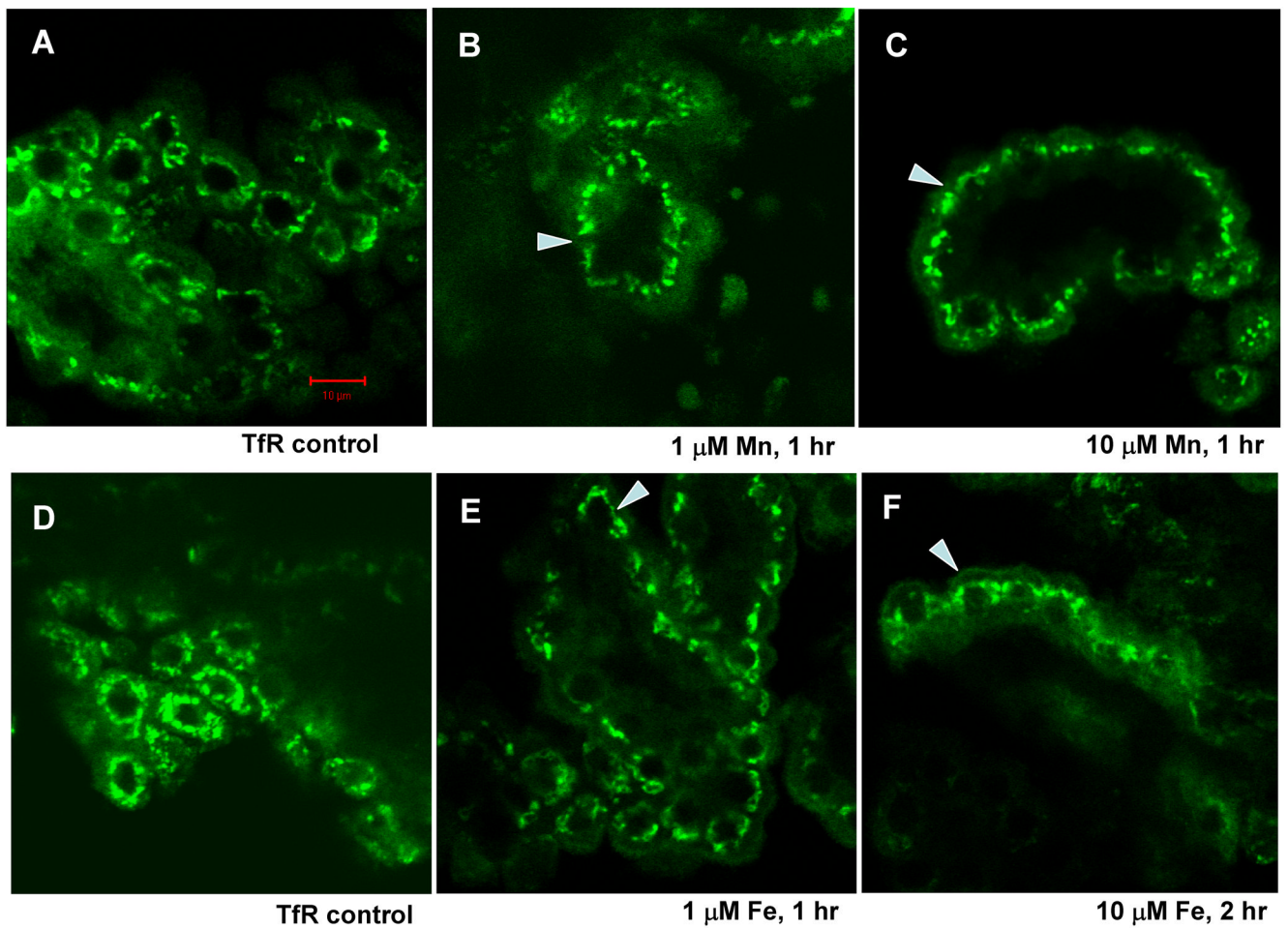


Fig. 4.

Confocal study of TfR cellular distribution in rat choroid plexus tissues as affected by treatment with 0, 1, and 10 μ M Mn (A, B, and C) or Fe (D, E and F) for 1 hr or 2 hr. Tissues were immunostained with anti-TfR antibody. With an increase in Mn concentrations, TfR stains moved toward the apical side of the choroidal epithelia, yet still seen closely to the nucleus. Incubation with Fe resulted in the similar redistribution of MTP1. Long exposure (2 hrs) did not move TfR further to the apical side. Arrows indicated TfR redistribution of in response to Mn or Fe.

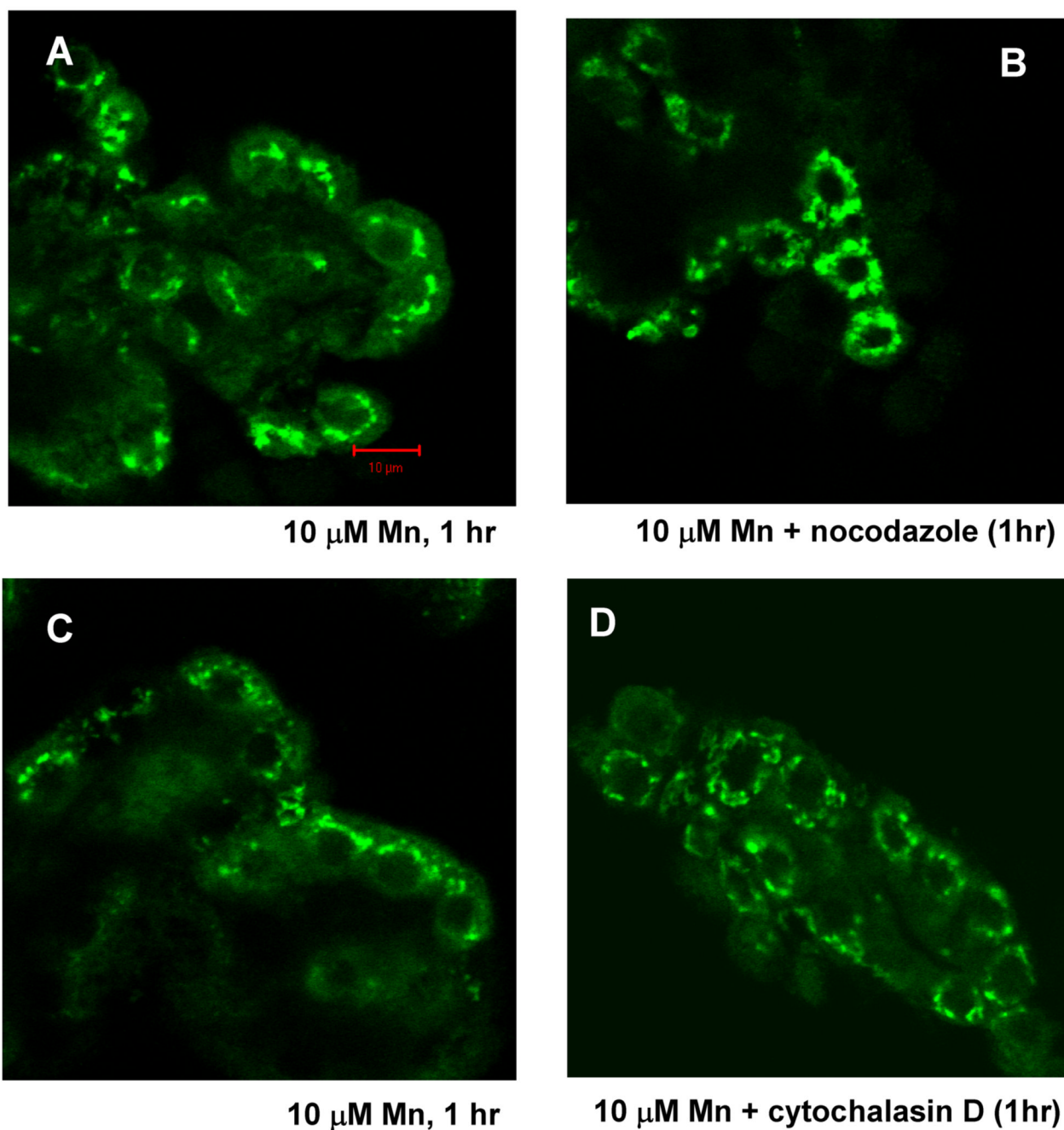


Fig. 5. Microtubule inhibitor-nocodazole eliminates TfR redistribution as affected by Mn or Fe treatment in rat choroid plexus tissues, so does microfilament inhibitor-cytochalasin D. Confocal study showed TfR cellular redistribution in rat choroid plexus tissues as affected by treatment with 10 μM Mn (A and C) for 1 hr. Pre-treatment of nocodazole (10μM, 1 hr) and cytochalasin D (1μM, 1 hr) blocked Mn- induced redistribution (B and D).

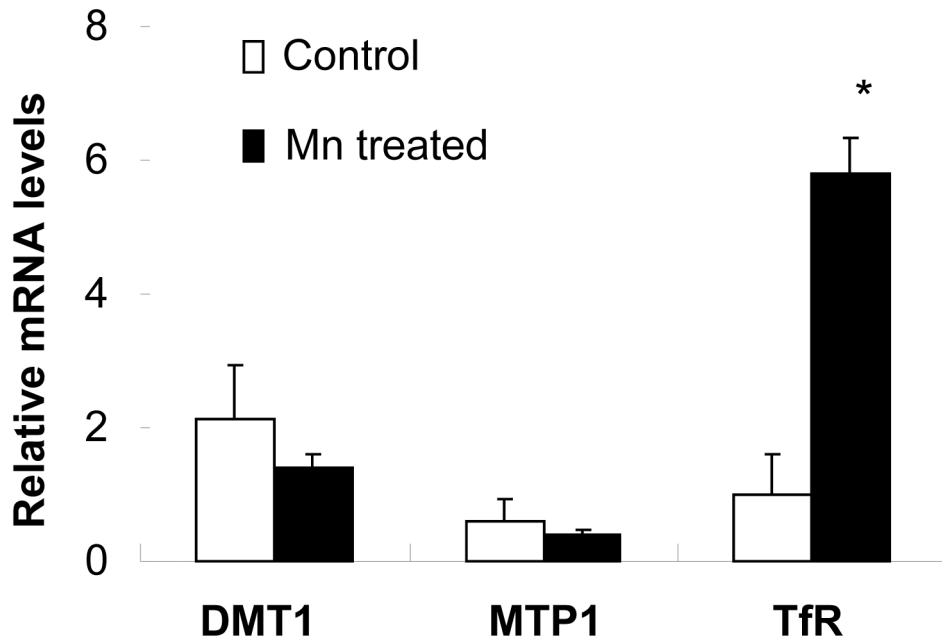
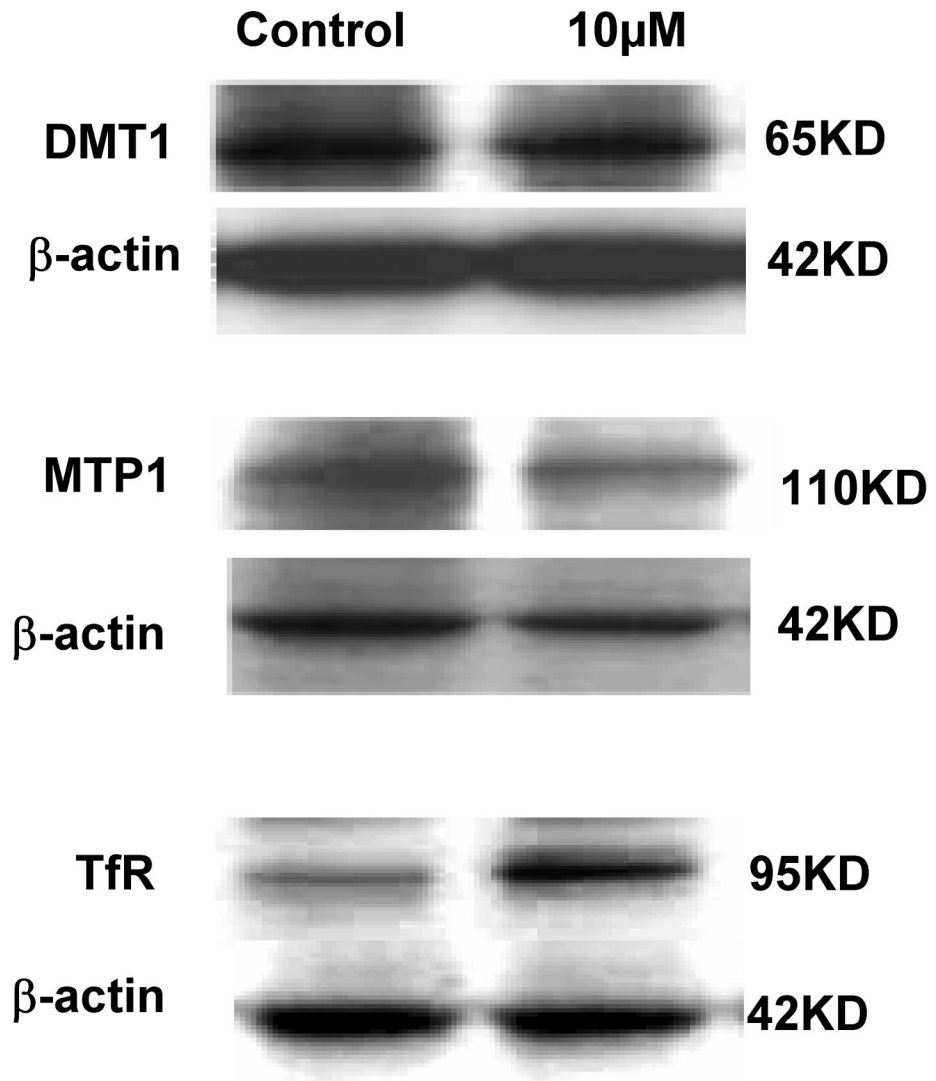


Fig. 6. Expression of DMT1, MTP1 or TfR mRNA in rat choroid plexus tissues as affected by Mn exposure. The choroid plexus tissues were incubated with 10 μ M Mn for 1hr. The relative mRNA levels of DMT1, MTP1, TfR and GAPDH were quantified by real-time RT-PCR and expressed as the ratio of DMT1/GAPDH, MTP1/GAPDH or TfR/GAPDH. Data represent mean \pm SE, n=3; *: p<0.01 as compared to control.



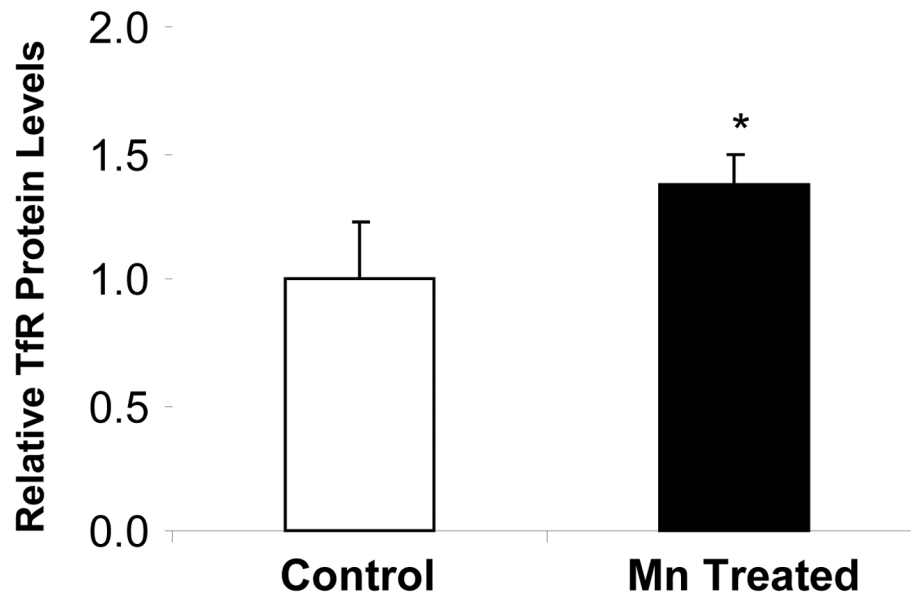


Fig. 7.

Expression of DMT1, MTP1 or TfR proteins in rat choroid plexuses as affected by Mn exposure. The choroid plexus tissues were incubated with 10 μ M Mn for 1 hr. The Western blots (A) are representative of triplicate experiments. The relative protein levels of TfR (B) were estimated from the corresponding band densities and normalized to those of β -actin. Data represent mean \pm SE, n=3; p<0.05 as compared to control.

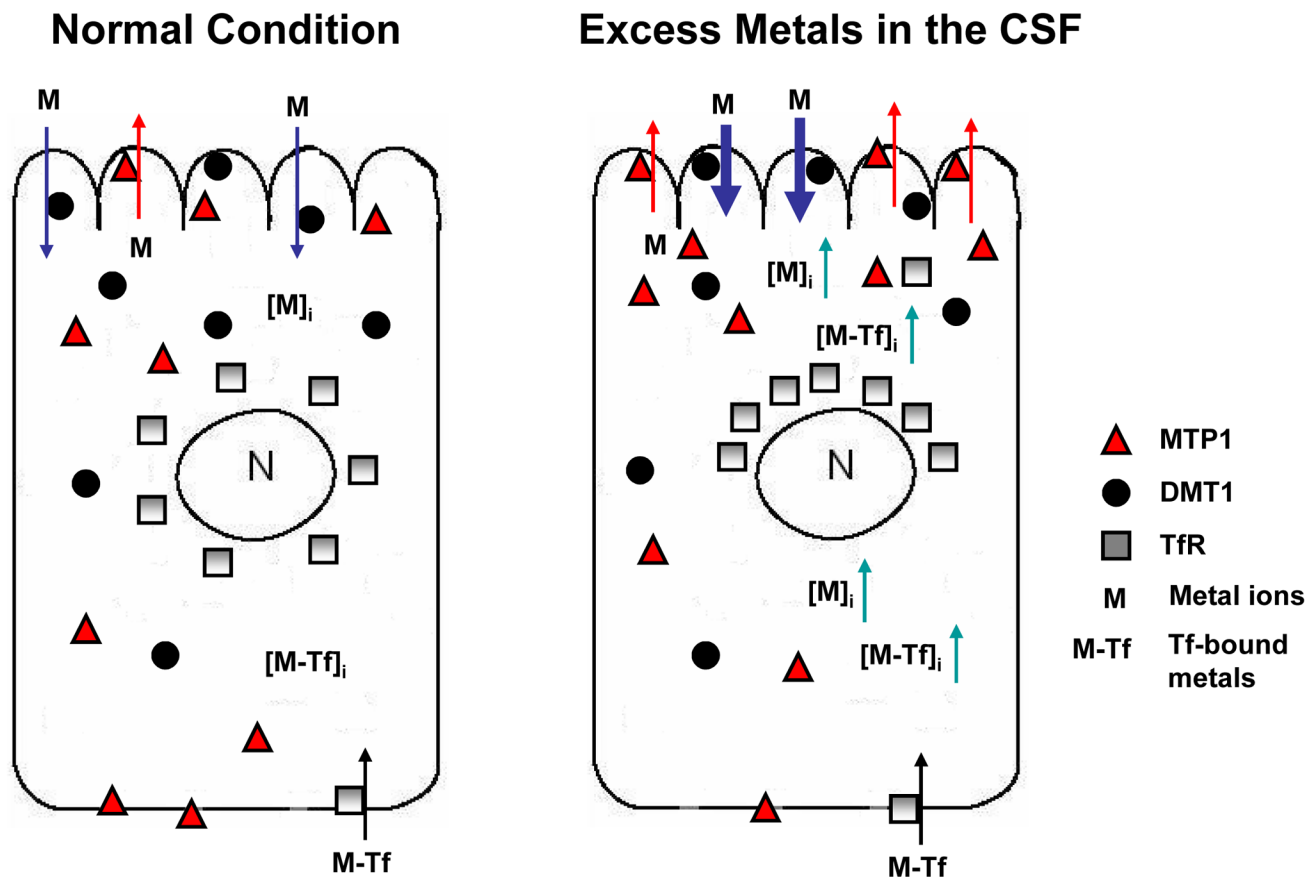


Fig. 8. Metal transport by MTP1, DMT1 and TfR in choroidal epithelial cells. Under physiological condition, DMT1 takes up Mn or Fe from the CSF, while MTP1 expels metals to the CSF. Upon metal exposure from the CSF, the uptake of metals by apical DMT1 increases intracellular metal concentrations. MTP1, in response, moves toward apical microvilli, expelling metal ions back to the CSF. Elevated Mn concentration enhances the translational expression of TfR, leading to a TfR-mediated transport of transferrin-bound metals including Fe to the CSF.